MATERIALE PLASTICE
https://revmaterialeplastice.ro
https://doi.org/10.37358/Mat.Plast.1964

Injectable Self-Healing Hydrogel for Localized Delivery of N-Acetylcysteine to Promote Airway Epithelial Repair

WENSEN YAN[1,#], CANHONG GAO[2,#], SUJUN CHEN[1], SENPENG FANG[2*]
[1] Pulmonary and Critical Care Medicine, Guangdong Second Provincial General Hospital, Guangzhou, 510317, China
[2] Pulmonary and Critical Care Medicine, Huilai County People's Hospital, Jieyang, 515200, China

Abstract: ***Background:*** *Airway epithelial injury is common in respiratory diseases and post-surgical conditions, leading to impaired barrier function and delayed healing. There remains an urgent need for localized biomaterial-based therapies to support epithelial repair under oxidative stress.* ***Methods:*** *We developed a self-healing injectable hydrogel based on chitosan and oxidized dextran, crosslinked via dynamic imine bonds. N-acetylcysteine (NAC) was encapsulated as a therapeutic payload. The hydrogel was characterized for rheological recovery, drug release kinetics, and evaluated in vitro using airway epithelial cells.* ***Results:*** *The hydrogel exhibited excellent self-healing behavior and sustained NAC release over 48 h. It promoted cell proliferation, enhanced migration in scratch assays, and upregulated ZO-1 expression. In an H_2O_2-induced injury model, NAC-loaded hydrogels significantly restored cell viability to near-normal levels.* ***Conclusion:*** *This NAC-loaded self-healing hydrogel provides both mechanical and biochemical support for airway epithelial repair. It offers a minimally invasive platform for localized treatment of airway injuries, with potential applications in respiratory disease management and post-operative mucosal healing.*

Keywords: *Self-healing hydrogel, airway epithelial repair, chitosan, oxidized dextran, N-acetylcysteine, dynamic covalent crosslinking, drug delivery*

1. Introduction

The airway epithelium plays a critical role as the first-line defense against inhaled pathogens, particulates, and environmental toxins. Integrity of the epithelial barrier is essential for mucociliary clearance and immune homeostasis [1,2]. However, in various respiratory diseases—including asthma, chronic obstructive pulmonary disease (COPD), and post-surgical trauma—this epithelial barrier is often disrupted, leading to impaired function, persistent inflammation, and delayed healing [3–5]. Effective restoration of epithelial continuity and tight junctions is therefore central to airway mucosal repair strategies [6,7].

Conventional treatments for airway injury primarily rely on systemic anti-inflammatory drugs and nebulized agents, which suffer from low localization efficiency, rapid clearance, and poor retention at the lesion site [8,9]. Localized biomaterial-based delivery platforms have emerged as promising alternatives, offering controlled drug release and microenvironmental support [10,11]. In particular, injectable hydrogels have received increasing attention due to their ability to fill irregular defects, conform to mucosal surfaces, and serve as carriers for therapeutic agents [12–14].

Self-healing hydrogels based on dynamic covalent chemistries offer unique advantages for airway applications [15,16]. Their reversible crosslinking allows rapid structural recovery under mechanical stress—an important feature for deployment in dynamic environments such as the respiratory tract [17,18]. Among various chemistries, Schiff base formation between amine and aldehyde groups has been widely employed for its mild reaction conditions and tunable gelation kinetics [19,20].

*email: fsp17875452730@163.com
[#] Equal Contribution: Wensen Yan, Canhong Gao

The airway mucosal surface is continuously exposed to airflow, mucus secretion, and ciliary clearance, which make local drug retention particularly challenging. Therefore, materials designed for airway delivery must not only provide sustained drug release but also maintain strong surface adhesion and structural stability under dynamic mechanical stress. Recent studies on local biomaterial delivery platforms have demonstrated that injectable, tissue-conformal, and self-healing hydrogels can overcome these challenges by adhering to mucosal tissues and resisting shear forces, thereby achieving prolonged residence and localized therapeutic efficacy [21]. Inspired by these principles, our hydrogel system was designed to form *in situ*, adhere intimately to the airway epithelium, and be well tolerated by epithelial cells without triggering irritation or cytotoxicity. Such features are crucial for ensuring stable retention and biocompatibility during airway epithelial repair. In this study, we report a dynamic imine-crosslinked injectable hydrogel composed of chitosan and oxidized dextran (ODex), designed for local airway delivery of N-acetylcysteine (NAC)—a clinically approved mucolytic and antioxidant agent. NAC has been widely used for respiratory indications due to its ability to scavenge reactive oxygen species (ROS), replenish intracellular glutathione, and modulate inflammation. However, its short half-life and poor mucosal retention limit its therapeutic efficacy in injured tissue [22,23].

Here, we hypothesize that an injectable NAC-loaded self-healing hydrogel can provide structural support and sustained biochemical stimulation to promote airway epithelial repair. We systematically evaluated the hydrogel's rheological properties, drug release behavior, and pro-regenerative effects using *in vitro* epithelial cell models. Assays were performed to assess cell viability, migration, tight junction protein expression (ZO-1), and oxidative injury recovery. This integrated platform may provide a minimally invasive, biomaterial-assisted strategy for treating airway epithelial damage in a wide range of clinical settings.

2. Materials and methods

2.1. Materials

Chitosan (degree of deacetylation ≥90%) and dextran (Mw ~100 kDa) were purchased from Macklin (Shanghai, China). Oxidized dextran (ODex) was prepared by reacting dextran with sodium periodate under dark conditions. N-acetylcysteine (NAC), hydrogen peroxide (H_2O_2), CCK-8 reagent, and other standard biochemical reagents were obtained from Sigma-Aldrich unless otherwise specified. Human bronchial epithelial cells (BEAS-2B) were obtained from ATCC.

2.2. Rheological self-healing test

The self-healing ability of the hydrogel was evaluated by time-dependent rheological measurements using a rotational rheometer (TA DHR-2) with a 20 mm parallel plate at 25°C. The hydrogel was subjected to a step-strain program:

1% strain (300 s) → baseline modulus,

300% strain (300 s) → network disruption,

return to 1% strain (900 s) → modulus recovery.

The storage modulus (G′) and loss modulus (G″) were recorded over time. All samples were prepared by mixing 2% (w/v) chitosan and 2% (w/v) ODex at a molar ratio of 1:1.

2.3. In vitro NAC release assay

The release profile of NAC from the hydrogel was measured by incubating NAC-loaded hydrogels (200 µL each) in 2 mL PBS (pH 7.4) at 37°C. At predetermined time points (0–48 h), 1 mL supernatant was collected and replaced with fresh PBS. The NAC concentration was quantified using UV–Vis spectrophotometry at 210 nm. All experiments were performed in triplicate, and cumulative release (%) was calculated.

2.4. Cell viability (CCK-8 assay)

BEAS-2B cells were seeded into 96-well plates (5×10^3 cells/well) and incubated overnight.

After 24, 48, and 72 h, CCK-8 reagent (10 μL/well) was added, and cells were incubated for 2 h. Absorbance at 450 nm was measured. Cell viability was normalized to the control group and reported as mean ± SD (n = 5).

2.5. Cell migration (scratch assay)

BEAS-2B cells were seeded into 6-well plates and cultured to ~90% confluency. A sterile pipette tip was used to scratch the cell monolayer to form a straight wound. After washing with PBS, cells were treated with Control medium, Gel, or Gel+NAC hydrogel-conditioned medium. After 24 h, wound closure was visualized under an inverted microscope (100×), and representative images were collected. Cell morphology, migration, and fluorescence staining were observed using an inverted fluorescence microscope (Olympus IX73, Olympus Corporation, Japan). Images were captured under identical exposure settings for all groups. A scale bar of 200 μm was included in each image. Quantitative image analyses, including scratch width and fluorescence intensity, were performed using ImageJ (NIH, USA) by two independent researchers in a blinded manner.

2.6. ZO-1 immunofluorescence and quantification

Cells treated as above were fixed with 4% paraformaldehyde, permeabilized with 0.1% Triton X-100, and blocked with 5% BSA. ZO-1 expression was visualized using anti–ZO-1 primary antibody (1:200) followed by Alexa Fluor–conjugated secondary antibody. Nuclei were counterstained with DAPI. Images were acquired by fluorescence microscopy and analyzed using ImageJ for relative fluorescence intensity. Data are expressed as % of control (n = 3).

2.7. Oxidative injury and viability rescue

To model oxidative injury, BEAS-2B cells were incubated with 300 μM H_2O_2 for 2 h. After washing, after 24 h of incubation, CCK-8 assay was performed as described above. Viability was expressed relative to untreated, undamaged control cells (set as 100%).

All quantitative data are presented as mean ± standard deviation (SD). Statistical analyses were performed using GraphPad Prism 9.0 (GraphPad Software, USA). Differences among groups were evaluated by one-way ANOVA followed by Tukey's post-hoc test. A value of $p < 0.05$ was considered statistically significant, and the levels of significance are indicated in the figures as follows:
$p < 0.05$ (*), $p < 0.01$ (**), $p < 0.001$ (***), $p < 0.0001$ (****).

Each experiment was independently repeated at least three times (n = 3), and the number of replicates is indicated in the corresponding figure legends.

3. Results

As shown in Figure 1, a chitosan/oxidized dextran-based injectable self-healing hydrogel was designed to deliver N-acetylcysteine (NAC) for epithelial repair. The hydrogel forms rapidly at the site of injury via dynamic Schiff base crosslinking, conforming to the lesion geometry. NAC, a known antioxidant and anti-inflammatory agent, is encapsulated within the hydrogel and released gradually to exert protective and pro-regenerative effects. This schematic depicts the sequential events following hydrogel administration: lesion filling, sustained drug release, directional cell migration, and wound closure. These processes are supported by *in vitro* results presented in following results, which demonstrate enhanced cell viability, migration, and tight junction restoration in NAC-loaded hydrogel-treated groups.

Figure 2 presents the rheological response of the chitosan/oxidized dextran hydrogel under a step-strain recovery test, designed to evaluate its self-healing behavior. When subjected to a high strain (300%), the hydrogel's internal network was disrupted, as evidenced by a rapid drop in the storage modulus (G′) from ~1000 to ~400 Pa. Upon restoring the strain to 1%, G′ gradually recovered over 900 s, reaching approximately 90% of its original value. Throughout the test, the loss modulus (G″) remained lower than G′, indicating the hydrogel maintained an elastic-dominant character. These results

confirm the self-healing property of the hydrogel, driven by reversible Schiff base linkages between amino groups on chitosan and aldehyde groups on oxidized dextran.

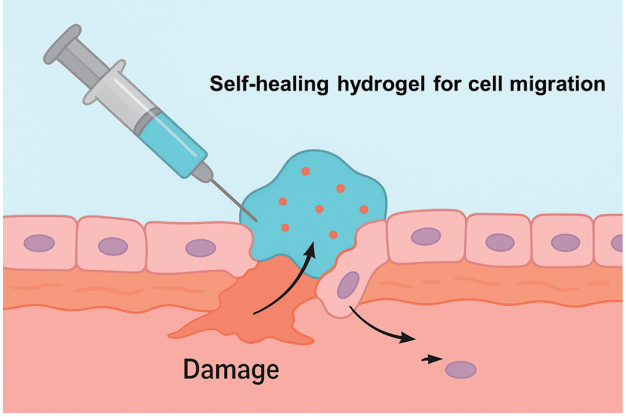

Figure 1. Schematic illustration of an injectable self-healing chitosan-based hydrogel delivering N-acetylcysteine (NAC) to promote airway epithelial repair. Upon injection at the injury site, the dynamic imine-crosslinked hydrogel forms *in situ*, releasing NAC locally. This facilitates epithelial cell migration and coverage of the damaged region, ultimately supporting restoration of the epithelial barrier

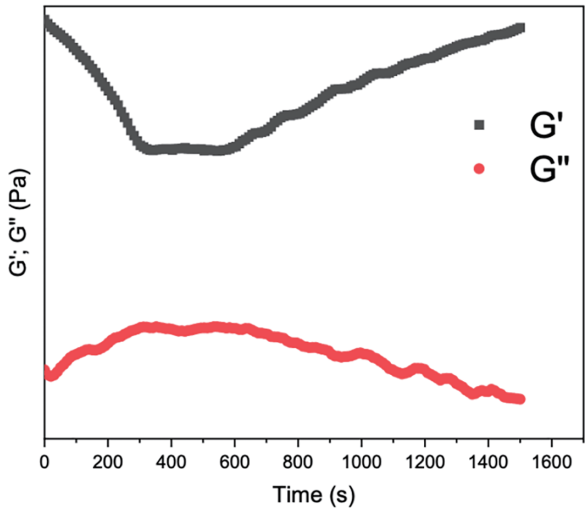

Figure 2. Time-dependent recovery of storage modulus (G′) and loss modulus (G″) of the chitosan/oxidized dextran hydrogel under step-strain conditions. Upon exposure to high strain (300%) to disrupt the network, the hydrogel's G′ sharply decreased. When returned to low strain (1%), G′ gradually recovered to near-initial levels, confirming the hydrogel's dynamic self-healing capability based on reversible imine crosslinking

As shown in Figure 3, the release behavior of NAC from the dynamic covalent chitosan/oxidized dextran hydrogel was characterized over a 48-h period. The hydrogel demonstrated a biphasic release pattern: an initial burst within the first 8 h, reaching ~80% release, followed by a slower, sustained release phase that plateaued around 95%. This profile suggests that NAC molecules were partially distributed near the hydrogel surface (leading to the burst phase), while the remainder was embedded

deeper in the network, resulting in prolonged diffusion-controlled release. The release kinetics ensured continuous exposure of NAC to surrounding cells in subsequent *in vitro* assays.

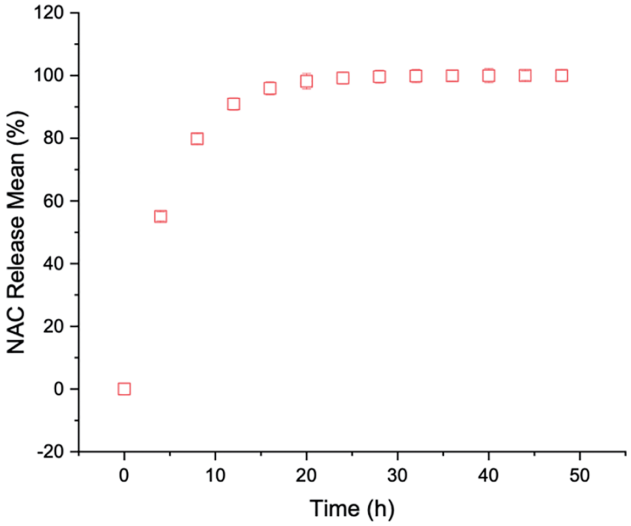

Figure 3. Cumulative release profile of N-acetylcysteine (NAC) from the chitosan/oxidized dextran hydrogel over 48 h. The hydrogel exhibited a rapid initial release phase within the first 8 h, followed by a sustained and gradual release plateauing near 95%, indicating stable network retention and drug release capacity

Figure 4 shows the quantitative results of cell viability measured at 24, 48, and 72 h using the CCK-8 assay. Compared with the control group, both the blank hydrogel (Gel) and NAC-loaded hydrogel (Gel+NAC) groups promoted epithelial cell proliferation over time. The Gel+NAC group exhibited a more pronounced increase in viability, with values reaching ~170% at 72 h, significantly higher than both the control and blank Gel groups. These findings suggest that the dynamic hydrogel provides a biocompatible environment conducive to cell survival, and the sustained release of NAC further enhances cellular proliferation.

Figure 5 displays representative images of a scratch assay performed to assess the impact of hydrogel treatment on airway epithelial cell migration. In the control group, the scratch gap remained wide after 24 h, indicating limited spontaneous migration. In contrast, the Gel group exhibited moderate closure of the wound area, suggesting that the hydrogel matrix provides a favorable environment for migration. Notably, the Gel+NAC group showed a nearly complete closure of the scratch, demonstrating significantly enhanced migration. These results suggest that both the hydrogel structure and the therapeutic NAC content synergistically promote epithelial cell motility and wound repair.

Figure 6 presents the quantification of the tight junction protein ZO-1 in airway epithelial cells after treatment with blank hydrogel (Gel) or NAC-loaded hydrogel (Gel+NAC). ZO-1 expression was assessed via immunofluorescence staining and normalized to the untreated control group (set at 100%). Treatment with Gel led to a ~30% increase in ZO-1 levels, whereas Gel+NAC significantly upregulated expression to ~165%. This result indicates that the hydrogel matrix, particularly when combined with NAC, enhances epithelial tight junction integrity.

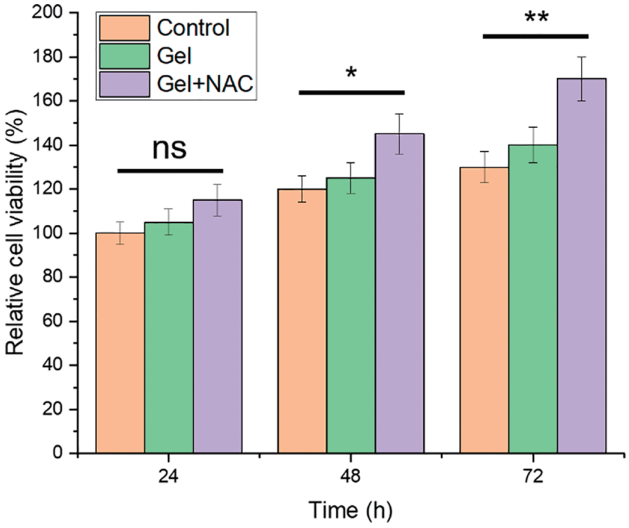

Figure 4. Effects of hydrogel and NAC-loaded hydrogel on airway epithelial cell viability at 24, 48, and 72 h. Cell viability was measured by CCK-8 assay and expressed as a percentage relative to the control group (set as 100%). Both hydrogel groups enhanced cell viability over time, with the Gel+NAC group showing significantly higher viability at all time points, $p > 0.05$ (ns), $^{*}p < 0.05$, $^{**}p < 0.01$

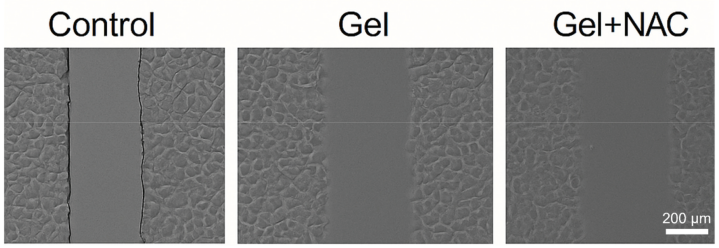

Figure 5. Representative microscopic images of airway epithelial cell migration assessed by scratch assay after 24 h. Compared with the untreated control, both Gel and Gel+NAC groups exhibited enhanced wound closure, with Gel+NAC showing the most significant reduction in scratch width

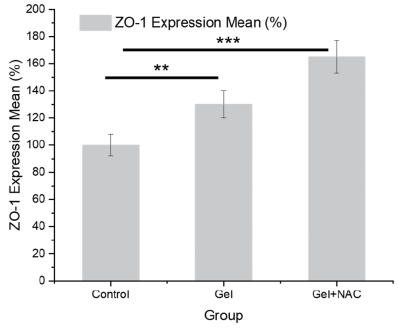

Figure 6. Quantification of ZO-1 expression in airway epithelial cells after treatment with hydrogel or NAC-loaded hydrogel. ZO-1 levels were measured by immunofluorescence and normalized to the control group. Both Gel and Gel+NAC groups showed enhanced expression, with the Gel+NAC group displaying the highest increase, $^{**}p < 0.01$, $^{***}p < 0.001$

Figure 7 shows the cell viability data of epithelial cells (likely BEAS-2B or similar) cultured with the different experimental treatments, including the control, gel-only, and Gel+NAC conditions. The data clearly demonstrates that cells treated with Gel+NAC exhibit a significant increase in viability compared to both the control and Gel-only groups at the corresponding time points. This suggests that the presence of NAC within the hydrogel formulation provides a notable cytoprotective effect, likely through its antioxidant properties. In contrast, the Gel-only group also showed some enhancement over the control, highlighting the potential structural or supportive effects of the hydrogel itself, though the Gel+NAC group consistently showed superior performance.

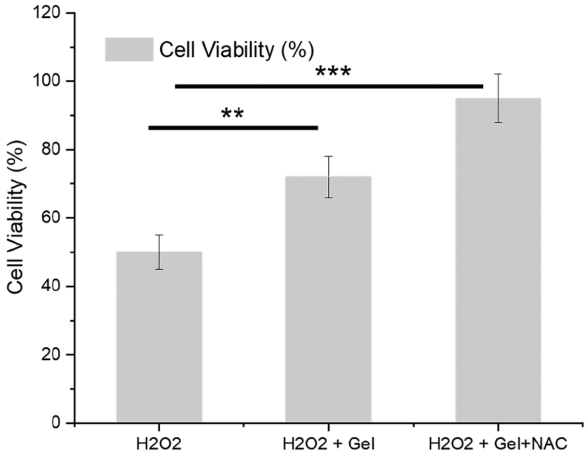

Figure 7. Restoration of cell viability in H_2O_2-damaged airway epithelial cells after treatment with hydrogel or NAC-loaded hydrogel. Viability was assessed by CCK-8 assay and expressed as a percentage relative to the undamaged control. Both Gel and Gel+NAC treatments significantly restored viability, with the Gel+NAC group approaching near-complete recovery, $^{**}p < 0.01$, $^{***}p < 0.001$

4. Discussion

Figure 1 highlights the conceptual framework of using a dynamic imine-crosslinked hydrogel for airway epithelial regeneration. The injectable hydrogel system, formed by mixing amino-rich chitosan and aldehyde-functionalized dextran (oxidized dextran), enables self-healing via reversible Schiff base bonds, ensuring structural continuity even under airway mechanical stress. The local delivery of NAC addresses oxidative injury by scavenging reactive oxygen species and inhibiting inflammatory signaling pathways. Furthermore, NAC promotes epithelial cell proliferation and migration, crucial for mucosal recovery. The hydrogel's injectability, self-repairing ability, and therapeutic payload make it well-suited for localized treatment of epithelial injuries caused by trauma, surgery, or chronic inflammation. Overall, this platform combines mechanical adaptability and biochemical support to enhance epithelial repair in a minimally invasive manner [24].

The biphasic release pattern of NAC observed in this study is a characteristic outcome of the dynamic imine-crosslinked chitosan/oxidized dextran network. The release rate can be readily modulated by adjusting several formulation parameters, such as the degree of oxidation of dextran, the chitosan-to-oxidized dextran ratio, and the total polymer concentration. Increasing crosslink density or polymer content yields a denser network with smaller pore size, thereby retarding diffusion and extending the sustained release phase. In contrast, a lower crosslink density allows greater chain mobility and accelerates the initial burst.

Such tunability is therapeutically significant for airway repair. The initial burst release provides rapid NAC delivery to immediately scavenge reactive oxygen species and attenuate acute inflammatory

signaling at the injury site. This early-phase antioxidant protection is critical to preserve epithelial cell viability and prevent further tissue damage. The subsequent sustained release phase ensures a prolonged local supply of NAC, maintaining a microenvironment that supports epithelial cell migration, proliferation, and tight-junction protein (ZO-1) upregulation, which collectively contribute to barrier restoration. Hence, rather than being a limitation, the biphasic release behavior represents an advantageous, controllable feature of the hydrogel system that aligns well with the temporal needs of airway mucosal healing.

The rheological recovery behavior shown in Figure 2 demonstrates that the chitosan/oxidized dextran hydrogel possesses excellent self-healing ability, critical for applications in dynamic environments such as the airway. The reversible drop and gradual restoration of G′ reflect the breakage and reformation of imine bonds under cyclic strain, a hallmark of dynamic covalent crosslinked systems [25]. This feature ensures that the hydrogel can maintain mechanical integrity and adhesion at the tissue interface even after mechanical deformation (e.g., during coughing or airflow) [26]. Moreover, this self-healing behavior contributes to the long-term stability and sustained therapeutic effect of the hydrogel system, supporting its use as a smart, minimally invasive material for epithelial tissue repair [27].

The self-healing behavior of the hydrogel plays a critical role in maintaining its functional stability in the mechanically dynamic airway environment. During respiration or coughing, the mucosal surface is repeatedly stretched and subjected to shear stress, which can lead to disruption of conventional hydrogels. The dynamic imine-crosslinked network described here allows rapid reconstruction of broken bonds, enabling the hydrogel to spontaneously recover its integrity and maintain close contact with the epithelial tissue. In this study, the endpoint of self-healing was defined as the recovery of the storage modulus (G′) to at least 90% of its initial value following high-strain deformation. This quantitative criterion indicates that the hydrogel can restore its internal crosslinked structure effectively, ensuring long-term mechanical stability and continuous drug release at the site of application.

The release kinetics of NAC from the self-healing hydrogel indicate that this system provides both immediate and sustained therapeutic delivery [28,29]. The initial burst release may be beneficial for neutralizing accumulated ROS and reducing acute oxidative stress at the injury site, while the sustained release supports long-term anti-inflammatory and epithelial repair processes. The dynamic imine-crosslinked network not only ensures mechanical adaptability (as shown in Figure 2), but also offers a diffusion-regulated matrix that preserves drug stability and avoids premature leakage [30]. Such a release profile is particularly favorable for treating airway injury, where both early intervention and prolonged support are required to prevent secondary damage and promote mucosal healing [31]. Beyond the initial 48 h, the hydrogel continues to release NAC at a low but steady rate due to the reversible nature of its dynamic covalent crosslinks. This prolonged release phase plays an essential role in maintaining a stable antioxidant microenvironment throughout the extended period of epithelial remodeling. Continuous exposure to NAC prevents secondary ROS accumulation, suppresses chronic inflammatory responses, and supports late-stage cellular activities such as proliferation, differentiation, and tight-junction stabilization. Therefore, the long-term release capacity of the chitosan/oxidized dextran hydrogel is not merely a kinetic feature but a critical determinant of durable airway barrier recovery. The therapeutic benefits of the hydrogel system are closely linked to the temporal profile of NAC release. The rapid burst phase ensures immediate antioxidant protection, neutralizing excessive ROS and alleviating acute oxidative damage to epithelial cells. This early response preserves cell viability and prevents apoptosis, creating a favorable foundation for tissue recovery. Subsequently, the sustained release phase maintains a moderate NAC concentration that continuously suppresses residual oxidative and inflammatory signaling. Such a stable redox environment promotes epithelial cell proliferation and migration, as well as the reassembly of tight junction proteins like ZO-1, which are essential for barrier restoration. Therefore, the sequential release of NAC not only provides chemical protection but also orchestrates the cellular events required for efficient airway epithelial regeneration.

The cell viability data in Figure 4 confirm the cytocompatibility and bioactivity of the chitosan/oxidized dextran hydrogel system. The hydrogel alone provided a favorable 3D matrix that supports epithelial adhesion and spreading. The additional incorporation of NAC further boosted cell viability, likely due to its antioxidant and cytoprotective effects under oxidative culture conditions. This is particularly relevant for epithelial repair, where cellular regeneration must be sustained in a ROS-rich microenvironment. The time-dependent enhancement observed here aligns with the NAC release profile (Figure 3), indicating that the therapeutic payload is delivered in a bioavailable and effective manner. Overall, these results demonstrate that the hydrogel platform not only supports cell growth but also enables pharmacologically active repair.

The scratch assay results in Figure 5 support the pro-migratory effect of the chitosan/oxidized dextran hydrogel, particularly when loaded with NAC. Cell migration is a critical step in epithelial wound healing, enabling re-epithelialization and restoration of barrier function. The enhanced closure observed in the Gel+NAC group is attributed to NAC's known ability to modulate oxidative stress, reduce inflammatory signaling, and promote cytoskeletal reorganization, all of which facilitate cell motility [32]. Additionally, the hydrogel's hydrated, permissive environment supports directional cell movement. These findings align with the viability data in Figure 4 and further confirm the regenerative potential of the hydrogel system in airway epithelial repair applications.

The increase in ZO-1 expression observed in Figure 6 highlights the potential of the hydrogel system to promote epithelial barrier reconstruction. ZO-1 is a key tight junction protein involved in maintaining the selective permeability and structural integrity of epithelial layers. Upregulation of ZO-1 suggests not only improved cell–cell contact but also functional recovery of the epithelial barrier. The stronger effect seen in the Gel+NAC group is likely due to NAC's ability to suppress oxidative damage and inflammation, thereby facilitating tight junction reassembly. Together with the migration and viability data (Figures 4 and 5), this result supports the conclusion that the NAC-loaded self-healing hydrogel promotes both structural and functional repair of airway epithelial tissue.

The results presented in Figure 7 highlight the beneficial effects of NAC when delivered through the self-healing hydrogel system. The significant increase in cell viability observed in the Gel+NAC group compared to the control and Gel-only groups suggests that NAC, when delivered in a sustained and localized manner via the hydrogel, exerts protective effects against cellular oxidative stress, which is commonly induced in the context of airway epithelial injury.

While the Gel-only group shows a modest improvement in cell viability compared to the control, this indicates that the hydrogel itself may provide some mechanical support or protective effects, such as by preventing cell detachment or promoting cell adhesion. However, it is clear that the presence of NAC enhances the cellular response beyond the matrix's physical effects alone. NAC, as an antioxidant, likely scavenges reactive oxygen species (ROS) and alleviates oxidative stress, leading to improved cell survival. This is particularly relevant in the context of airway epithelial repair, where oxidative damage often contributes to tissue injury and delayed healing.

The combination of the self-healing hydrogel matrix and NAC's antioxidant properties provides a dual mechanism to promote cellular repair, making it a promising system for localized therapy in the airways. Further studies could explore the specific pathways involved, such as NAC's role in regulating ROS signaling or its interaction with tight junction proteins like ZO-1 to restore barrier function more effectively.

5. Conclusion

In this study, we developed a self-healing injectable hydrogel based on dynamic Schiff base crosslinking between chitosan and oxidized dextran for the localized delivery of N-acetylcysteine (NAC) to promote airway epithelial repair. The hydrogel exhibited excellent self-healing behavior, as confirmed by time-dependent rheological recovery, enabling it to maintain integrity under mechanical stress. *In*

vitro drug release assays demonstrated a biphasic release profile of NAC, providing both rapid and sustained therapeutic exposure.

Biocompatibility assessments showed that both the blank hydrogel and NAC-loaded hydrogel supported epithelial cell viability, with the NAC formulation significantly enhancing proliferation. Scratch assays revealed that the hydrogel system promoted epithelial migration, particularly in the presence of NAC. Furthermore, immunofluorescence quantification indicated that ZO-1 expression, a key marker of epithelial tight junction integrity, was markedly upregulated in the hydrogel-treated groups. Finally, under oxidative stress induced by H_2O_2, the NAC-loaded hydrogel effectively restored cell viability, highlighting its protective capability in injury-mimicking environments.

Collectively, these findings demonstrate that the chitosan/oxidized dextran self-healing hydrogel is a promising platform for airway epithelial regeneration, offering injectability, mechanical adaptability, and controlled drug delivery. This system provides a minimally invasive strategy for enhancing mucosal healing in respiratory diseases and post-surgical repair.

Acknowledgement: Not applicable.

Funding Statement: The authors declare that they have received no funding.

Author Contributions: All authors contributed to this present work: Wensen Yan designed the study, Sujun Chen acquired the data, Canhong Gao interpreted the data, Senpeng Fang drafted the manuscript and revised the manuscript. All authors reviewed the results and approved the final version of the manuscript.

Availability of Data and Materials: The datasets generated or analyzed during the current study are available from the corresponding author Senpeng Fang upon reasonable request.

Ethics Approval: Not applicable.

Conflicts of Interest: The authors declare no conflicts of interest to report regarding the present study.

Abbreviations

NAC	N-acetylcysteine
ZO-1	Zonula Occludens-1
COPD	Chronic obstructive pulmonary disease
ODex	Oxidized dextran
Reactive oxygen species	Reactive oxygen species
BEAS-2B	Bronchial Epithelial Cell line
BSA	Bovine Serum Albumin

References

1. Michael S, Liotta N, Fei T, Bendall ML, Nixon DF, Dopkins N. Endogenous retroelement expression in modeled airway epithelial repair. Micr Infect. 2024;27(5–6):105465. doi:10.1016/j.micinf.2024.105465.
2. Hu DJ-K, Cai XT, Simons J, Yun J, Elstrott J, Jasper H. Non-canonical Wnt signaling promotes epithelial fluidization in the repairing airway. Nat Commun. 2025;16(1):4124. doi:10.1038/s41467-025-59320-1.
3. McGraw MD, Yee M, Kim S-Y, Dylag AM, Lawrence BP, O'Reilly MA. Diacetyl inhalation impairs airway epithelial repair in mice infected with influenza A virus. Am J Physiol-Lung Cellu Molecu Physiol. 2022;323(5):L578–92. doi:10.1152/ajplung.00124.2022.
4. Liu X, Bai Y, Zhao X, Chen J, Chen X, Yang W. Conductive and self-healing hydrogel for flexible electrochemiluminescence sensor. Microchimica Acta. 2023;190(4):123. doi:10.1007/s00604-023-05706-1.

5. Heijink IH, Nwozor KO, Hackett T-L. Closing the gap: use of polidocanol to study human airway epithelial repair. Am J Respirat Cell Molec Biol. 2025;73(5):643–5. doi:10.1165/rcmb.2025-0165ed.
6. Bequignon E, Mangin D, Bécaud J, Pasquier J, Angely C, Bottier M, et al. Pathogenesis of chronic rhinosinusitis with nasal polyps: role of IL-6 in airway epithelial cell dysfunction. J Translat Med. 2020;18(1):136. doi:10.1186/s12967-020-02309-9.
7. Evans DJ, Smith EF, Hemy NR, Gibbons JTD, Wilson AC, Kicic A, et al. Delayed airway epithelial repair is correlated with airway obstruction in young adults born very preterm. ERJ Open Res. 2025;11(2):00816-2024. doi:10.1183/23120541.00816-2024.
8. Nie M, Kong B, Chen G, Xie Y, Zhao Y, Sun L. MSCs-laden injectable self-healing hydrogel for systemic sclerosis treatment. Bioact Mater. 2022;17:369–78. doi:10.1016/j.bioactmat.2022.01.006.
9. Muchlis AMG, Yang C, Tsai Y-T, Ummartyotin S, Lin CC. Multiresponsive self-healing lanthanide fluorescent hydrogel for smart textiles. Acs Appl Mat Interf. 2023;15(39):46085–97. doi:10.1021/acsami.3c10662.
10. Li B, Li Z, Li H. Ultrastretchable luminescent nanocomposite hydrogel with self-healing behavior. Acs Appl Polymer Mat. 2022;4(4):2329–36. doi:10.1021/acsapm.1c01531.
11. Karati D, Kumar D. Molecular insight into the apoptotic mechanism of cancer cells: an explicative review. Current Molec Pharmacol. 2024;17:e18761429273223. doi:10.2174/0118761429273223231124072223.
12. D'Souza A, Marshall LR, Yoon J, Kulesha A, Edirisinghe DIU, Chandrasekaran S, et al. Peptide hydrogel with self-healing and redox-responsive properties. Nano Converg. 2022;9(1):18. doi:10.1186/s40580-022-00309-7.
13. Chen J, Lin A, Luo P. Advancing pharmaceutical research: a comprehensive review of cutting-edge tools and technologies. Curr Pharm Anal. 2024;21(1):1–19. doi:10.1016/j.cpan.2024.11.001.
14. Chakraborty A, Zöller M, Sardogan A, Klotz M, Mastalerz M, Marchi H, et al. Development of a polidocanol-based human *in vitro* model to explore airway epithelial repair. Am J Respir Cell Mol Biol. 2025;73(5):668–85. doi:10.1165/rcmb.2024-0117oc.
15. Cadamuro F, Ardenti V, Nicotra F, Russo L. Alginate-gelatin self-healing hydrogel produced via static-dynamic crosslinking. Molecules. 2023;28(6):2851. doi:10.3390/molecules28062851.
16. Delesky EA, Jones RJ, Cook SM, Cameron JC, Hubler MH, Srubar WV. Hydrogel-assisted self-healing of biomineralized living building materials. J Cleaner Product. 2023;418:138178. doi:10.1016/j.jclepro.2023.138178.
17. Bitounis D, Huang Q, Toprani SM, Setyawati MI, Oliveira N, Wu Z, et al. Printer center nanoparticles alter the DNA repair capacity of human bronchial airway epithelial cells. Nanoimpact. 2022;25(1):100379. doi:10.1016/j.impact.2022.100379.
18. Niu J, Wang J, Shi Y, Dong Z, Huang T, Dai X, et al. Customizable, self-healing, and biocompatible microLED-hydrogel integration displays. Nano Energy. 2024;129(Pt B):110074. doi:10.1016/j.nanoen.2024.110074.
19. Bayram C. Carboxymethyl chitosan-glycerol multi-aldehyde based self-healing hydrogel system. Int J Biol Macromol. 2023;239:124334. doi:10.1016/j.ijbiomac.2023.124334.
20. Bai X, Wang M, Chen Y, Wu L, Yu J, Luo Y. Synthesis and properties of self-healing hydrogel plugging agent. J Appl Polym Sci. 2024;141(9):e55005. doi:10.1002/app.55005.
21. Lee Y, Kim M, Kim N, Byun S, Seo S, Han JY. Injectable hydrogel systems for targeted drug delivery: from site-specific application to design strategy. Appl Sci. 2025;15:11599. doi:10.3390/app152111599.
22. Pan S, Zhu C, Wu Y, Tao L. Chitosan-based self-healing hydrogel: from fabrication to biomedical application. Polymers. 2023;15(18):3768. doi:10.3390/polym15183768.

23. Palit N, Suryavanshi P, Banerjee S. Self-healing mineralized hydrogel scaffolds for stretch-triggered dye release. Polym Adv Technol. 2024;35(2):e6318. doi:10.1002/pat.6318.
24. Raby KL, Michaeloudes C, Tonkin J, Chung KF, Bhavsar PK. Mechanisms of airway epithelial injury and abnormal repair in asthma and COPD. Front Immunol. 2023;14:1201658. doi:10.3389/fimmu.2023.1201658.
25. Serena Di V, Dennis KN, Chiara C, Maria F, Pieter SH, Elisabetta P. Cigarette smoke impairs airway epithelial wound repair: role of modulation of epithelial-mesenchymal transition processes and notch-1 signaling. Antioxidants. 2022;11(10):2018. doi:10.3390/antiox11102018.
26. Shao S, Zhang N, Specht GP, You S, Song L, Fu Q, et al. Pharmacological expansion of type 2 alveolar epithelial cells promotes regenerative lower airway repair. Proc Natl Acad Sci U S A. 2024;121(16):e2400077121. doi:10.1073/pnas.2400077121.
27. Wang F, Chen K, Yi X, Shen Y, Lin Y, Zhou Z. Self-healing memristors based on SA/PVA/STB hydrogel. J Mat Sci-Mat Elect. 2023;34(20):1520. doi:10.1007/s10854-023-10942-5.
28. Wang X, Weng L, Zhang X, Guan L, Li X. Constructing conductive and mechanical strength self-healing hydrogel for fiexible sensor. J SciAdv Mat Devices. 2023;8(3):100563. doi:10.1016/j.jsamd.2023.100563.
29. Zertuche-Arias T, Alatorre-Meda M, Rivero IA, Juárez P, Castro-Ceseña AB. N-acetylcysteine and pro-adrenomedullin dual-crosslinked gelatin-chitosan hydrogels with enhanced mechanical and mineralization performance. RSC Adv. 2025;15:22524–33. doi:10.1039/d5ra03349g.
30. Xuan H, Wu S, Jin Y, Wei S, Xiong F, Xue Y, et al. A bioinspired self-healing conductive hydrogel promoting peripheral nerve regeneration. Adv Sci. 2023;10(28):e2302519. doi:10.1002/advs.202302519.
31. Zhang X, Liang Y, Huang S, Guo B. Chitosan-based self-healing hydrogel dressing for wound healing. Adv Colloid Interface Sci. 2024;332:103267. doi:10.1016/j.cis.2024.103267.
32. Zhao Z, Li Y, Wang H, Shan Y, Liu X, Wu M, et al. Ultra-tough self-healing hydrogel via hierarchical energy associative dissipation. Adv Sci. 2023;10(27):e2303315. doi:10.26434/chemrxiv-2022-0mgq4.

Received: 28 August 2025; Accepted: 13 November 2025; Published: 31 December 2025